Environmental Science and Pollution Research (2022) 29:41992–42004
https://doi.org/10.1007/s11356-021-16730-0

RECENT TRENDS IN THE APPLICATION OF GREEN TECHNOLOGIES AND THEIR MANAGEMENT

# Assessment of some water quality parameters in the Red River downstream, Vietnam by combining field monitoring and remote sensing method

Trinh Thi Tham[1] · Trinh Le Hung[2] · Trinh Thi Thuy[1] · Vu Thi Mai[1] · Le Thi Trinh[1] · Chu Vu Hai[3] · Tu Binh Minh[4]

Received: 9 April 2021 / Accepted: 22 September 2021 / Published online: 5 October 2021


**Abstract**
The Red River is the largest river in northern Vietnam, and it serves as the main water source for production and human activities in the Red River Delta region. Cities and provinces located in the Red River Delta, for example, Hanoi, Nam Dinh, and Ha Nam, have experienced rapid economic growth with various large urban, industrial zones, and agricultural areas. As a result of urbanization and industrialization, surface water in this region has been contaminated by multiple anthropogenic sources. In this study, in addition to water quality assessment using WQI, we used the reflectance values of visible and near-infrared bands and in situ data to build a regression model for several water quality parameters. Among ten parameters examined, two parameters, including total suspended solids (TSS) and turbidity, were used to construct regression correlation models using the Sentinel-2 multispectral images. Our results can contribute useful information for comprehensive monitoring, evaluation, and management scheme of water quality in the Red River Delta. The application of this method can overcome the limitation of actual observation results that only reflect local contamination status and require a lot of sampling and laboratory efforts.

**Keywords** Water quality · Red River · Remote sensing · Sentinel-2

## Introduction

The Red River is the largest river in northern Vietnam. The river originates from Yunnan Province (China) and flows through several provinces and cities in Vietnam such as Lao Cai, Yen Bai, Phu Tho, Vinh Phuc, Hanoi, Hung Yen, Ha Nam, Nam Dinh, and Thai Binh, before emptying into the East Sea. The river is 1150 km long with 800 km of meander through steep mountains and highlands with violent and unpredictable swell during the rainy season (Luu et al. 2010; NAWAPI and MONRE 2016). When the river reaches the Red River Delta, it turns quiet and gentle at an elevation above sea level of about 3 m. The Red River Delta plays a vital role in socio-economic development with various historical and cultural values. In recent years, many extensive industrial parks and key economic regions have been built in this delta area. Improper emissions from industrial parks, livestock farms, and domestic sectors have caused significant impacts on the water quality of the Red River Delta. The 2018 Annual Report of the Ministry of Natural Resources and Environment showed that the water quality of the Red River had trended downwards over the last 30 years (MONRE 2018). This report summarized the results of surface water quality monitoring for the period from 2014 to 2018 at 23 sampling sites in the Vietnam Red River. According to this report, the annual water quality indexes (WQI) that were calculated declined from 2015 to 2018 at almost all monitoring points. However, the fixed monitoring points with a relatively long distance, from 10 to 45 km, have not fully represented the water quality in the

Responsible Editor: Xianliang Yi

✉ Trinh Thi Tham
ttham@hunre.edu.vn

✉ Tu Binh Minh
tubinhminh@gmail.com

[1] Faculty of Environment, Hanoi University of Natural Resources and Environment, Hanoi, Vietnam

[2] Le Quy Don Technical University, Hanoi, Vietnam

[3] Goshu Kohsan Vietnam Company, Hanoi, Vietnam

[4] Faculty of Chemistry, University of Science, Vietnam National University, Hanoi, Vietnam

area, especially the locations affected by local pollution sources. The water and sediment contamination with organic and inorganic pollutants in the delta has also been documented by several previous studies. For example, the water quality of the Red River downstream was assessed in 2015 by analyzing some physicochemical variables at five sampling sites at the main axis of the Red River (Ba Lat estuary, Thai Binh Province) and four distributaries of the Red River (Hoang et al. 2016). Almost analyzed parameters such as total dissolved solids (TDS), turbidity, $NO_2^-$, $NO_3^-$, and $NH_4^+$ were under the permitting limit values of the National Technical Regulation on Surface Water Quality for the irrigation purposes, waterway, and other purposes with low-quality water requirements quality (QCVN 08:2015, column B1). However, the concentrations of $PO_4^{3-}$ varied from 1.17 to 1.70 mg P/L that were from 3.9 to 5.7 times higher than the permissible limit QCVN 08:2015. The concentration of individual parameters in the short-term studies did not completely show the synergistic effects of polluted sources on water quality. Similarly, the average concentrations of some heavy metals (Mn, Cd, Cr, Cu, Ni, Pb, and Zn) in sediments collected from the Red River ranged from 0.35 to 806 ng/g dry weight (Nguyen et al. 2016). At several sites in the upper of the Red River, the enrichment factors (EF) of Cu, Cd, Pb, Ni, and Zn showed that heavy metal pollution in sediment was significantly high values.

Various water quality index (WQI) models have been applied to assess surface water quality. The WQI data derived from physical, chemical, and biological parameters can provide helpful information for governmental authorities to improve or construct environmental regulations (Shweta et al. 2013). The formulas for calculating the freshwater supplier WQI were designed by Horton to control the quality of water for workers (Horton 1965). Since then, some QWI models had been researched and developed to apply to assess the pollution level of different water sources such as groundwater (Brown et al. 1971; Alastal et al. 2015), lake water (Tsegaye et al. 2006), surface river water (Sargaonkar and Deshpande 2003; Liou et al. 2004), and inland water (CCME 2001). In Vietnam, the Ministry of Natural Resources and Environment has issued a decision no. 1460/QD-TCMT on promulgating a manual to calculate WQI. In this guideline, the multiplicative aggregate function was given to estimate scores for groups of water quality parameters. Some authors have assessed the water quality based on this guideline. Cao et al. (2020) combined the WQI and the comprehensive pollution index (CPI) to evaluate the Cau River water quality at 23 sampling locations. The WQI showed the high water quality fluctuation due to geographical areas and the impacts of pollution sources. The WQI was also used for water resource management in Kien Giang Province, Vietnam (Tran and Pham 2020). The different WQI values for each time of monitoring and seasonality have recommended water use purposes, including domestic use but needing appropriate treatment measures, use for irrigation purposes, and use for other suitable purposes. At the Red River downstream, a few previous studies have measured the concentration of some water quality parameters in a short section of the Red River without a comprehensive calculation of WQI. Meanwhile, regular WQI measurement for the Red River water will indicate the local impacts of pollution sources from the inland.

Traditional methods for monitoring water quality, including sampling and analysis of samples in the laboratory, often require expensive costs and time-consuming and a sizeable specialized workforce (Giardino et al. 2010; Yepez et al. 2018). In comparison, remote sensing technology has been widely used to monitor, evaluate, and predict water quality parameters with high accuracy and time and cost-saving (Gholizadeh et al. 2016). The capabilities of satellite images can be exploited to monitor different phenomena over large spatial scales, such as the surface of rivers (Ennaji et al. 2018). Many moderate resolution satellite images (e.g., Landsat, MODIS, Sentinel) could be fee-download to turn measurement of satellite radiances into water quality information through some processing. In this process, excluding or correcting atmospheric interference from near-land targets and analyzing water reflectance are essential steps to estimate water quality parameters such as chlorophyll-a (Chl-a), colored dissolved organic matter (CDOM), suspended particulate matter (SPM), or turbidity (Richter 2009; Knaeps et al. 2012; Kiselev et al. 2015). The remote sensing technique can serve as an efficient tool for collecting and mapping pollutant information from some geographical regions. Initial studies on the remote sensing application to monitor water quality mainly focused on the relationship between reflected spectrums obtained from satellite images and quality parameters measured by empirical methods (Ritchie et al. 1976; Chen et al. 1992; Dekker et al. 1996). Earlier studies have found linear relationships between spectral reflection and some parameters such as total suspended solids (TSS) and chlorophyll-a concentrations in surface water (Ritchie et al. 1987; Ritchie et al. 1990; Chen et al. 1991; Moran 1992). Optical satellite images at different resolutions were used to determine TSS concentrations in surface water (He 2008; Doxaran et al. 2007; Guzman and Santaella 2009). The use of spatial resolution multispectral data, Landsat-8, Landsat-7, and Sentinel-2 for water quality monitoring was carried out in two small lakes in Italy and Belgium (Bresciani et al. 2019). Cloud-free satellite images were converted into information about the concentration of Chl-a, turbidity, Secchi disk depth (SDD), and water temperature by using an image processing chain implementing physical methods. These forecast results were also compared with 23 data points on-site. In addition, satellite images obtained simultaneously from Sentinel-2B sensor and Landsat-8 sensor were processed to obtain the concentrations of the four parameters mentioned above in a hydroelectric reservoir in Brazil

(Pizani et al. 2020). The researchers also evaluated the potential of water quality monitoring using Sentinel-2 observations at the Sado Estuary, Portugal. The match-ups of in situ and satellite data of suspended particle concentrations showed Sentinel-2 is effective for monitoring some variables such as Chl-a in a high fluctuate system (Sent et al. 2021). The low operating costs of the free use of available remote sensing data have strongly prompted water management agencies to use it as a water quality assessment tool alongside field monitoring. In Vietnam, there have been a few studies using optical satellite image data to assess water quality in coastal areas in Quang Ninh Province and Hai Phong City (Ke et al. 2015), Tri An Lake in Dong Nai Province (Hung and Tarasov 2016), and West Lake in Hanoi (Ha et al. 2016). In general, most studies in Vietnam use Landsat medium resolution satellite images in estimating water quality parameters (Pham et al. 2018; Hung and Tarasov 2016; Nguyen et al. 2017a, 2017b). Some recent studies have used Sentinel-2 high spatial resolution satellite images in estimating chlorophyll-a content in river and lake areas in Vietnam (Nguyen et al. 2017a, 2017b).

In this study, the WQI calculation formulas guided in decision no. 1460/QD-TCMT were applied to assess the water quality in the downstream Red River area. High sampling density with one sample every approximately 4 km effectively helped determine the water quality affected by different pollution sources. At the same time, we use the Sentinel-2 sensor with high-resolution images to determine the instant minimum variation of water quality parameters. The results obtained by the Sentinel-2 sensors are compared with data measured in actual water samples to assess possible errors of the remote sensing method. The research results will be the scientific basis for managers to use Sentinel-2 remote sensing images for regular water quality forecasting in the entire Red River basin. Implementing on-site sampling programs to measure water quality parameters and their ecological effects in water bodies is often expensive and time-consuming. Furthermore, this is often not representative of the total area of interest. Remote sensing techniques that provide cost-effective systematic observations of an extensive water system will offer enormous advantages.

## Material and methods

### Study area and field monitoring data

A total of 30 surface water samples were collected along the Red River in March 2019, from Hanoi City (20° 0′ 13″ N; 105° 52′ 50″ E) to Nam Dinh Province (20° 19′ 45″ N; 106° 15′ 43″), with 114.6 km in length (Fig. 1 and see Table S1 for more detail). The information about the distribution of the population and pollution sources in the study area is described in Table 1. All the samples were preserved from the change of composition due to various chemicals reactions, physical processes, and biodegradation (Sliwka-Kaszyńska et al. 2003). The analysis of physicochemical parameters such as total suspended solids (TSS), chemical oxygen demand (COD), chloride ($Cl^-$), ammonium ($NH_4^+$), nitrite ($NO_2^-$), nitrate ($NO_3^-$), phosphate ($PO_4^{3-}$), and arsenic (As) was performed according to the Vietnam Standards (TCVN) methods and the Standard Methods for the Examination of Water and Wastewater (SMEWW) (Baird et al. 2017). The pH, oxygen reduction potential (ORP), dissolved oxygen (DO), and conductivity parameters were measured in situ by using the multi-parameter meter (Hach HQ440D). These parameters were defined as water quality indicators following the National Technical Regulation on Surface Water Quality (QCVN 08-MT:2015/BTNMT).

Furthermore, to describe overall the quality of surface water used for different purposes, it is common to use the water quality index (WQI). In this study, the water quality index was calculated based on analysis results and applied the formulas given in no. 1460/QĐ-TCMT that were promulgated as technical guidelines for the calculation and publication of Vietnam's water quality index. Three groups among five groups of parameters have been selected for the total of WQI, including group 1 (pH values), group 3 (as was selected from the heavy metal group in this study), and group 4 (organic and nutrient parameters such as DO, turbidity, TSS, COD, $BOD_5$, $Cl^-$, $NO_3^-$, $NO_2^-$, $NH_4^+$, and $PO_4^{3-}$). The calculating WQI of the water body follows some equation bellowing:

$$WQI_{SI} = \frac{q_i - q_{i+1}}{BP_{i+1} - BP_i} * \left(BP_{i+1} - C_p\right) + q_{i+1} \quad (1)$$

$$WQI_{SI} = \frac{q_{i+1} - q_i}{BP_{i+1} - BP_i} * \left(C_p - BP_i\right) + q_i \quad (2)$$

where

$BP_i$ the lower limit concentration of the observed parameter specified in decision no. 1460/QĐTCMT corresponding to the level ($i$) (see Table S2-S5);

$BP_{i+1}$ the upper limit concentration of the observed parameter specified in decision no. 1460/QĐ-TCMT corresponding to the level ($i$+1) (see Table S2-S5);

$q_i$ WQI value corresponding to the level ($i$) specified in decision no. 1460/QĐ-TCMT (see Table S2-S5);

$q_{i+1}$ WQI value corresponding to the level ($i$ +1) specified in decision no. 1460/QĐ-TCMT (see Table S2-S5);

$C_p$ concentration of observed parameter selected for calculation.

Equation (1) is applied to calculate the sub-index of quality rating for most parameters. Equation (2) is used to calculate the quality rating for DO and pH in case the percentages of saturated DO range from 20 to 80% and pH values vary from

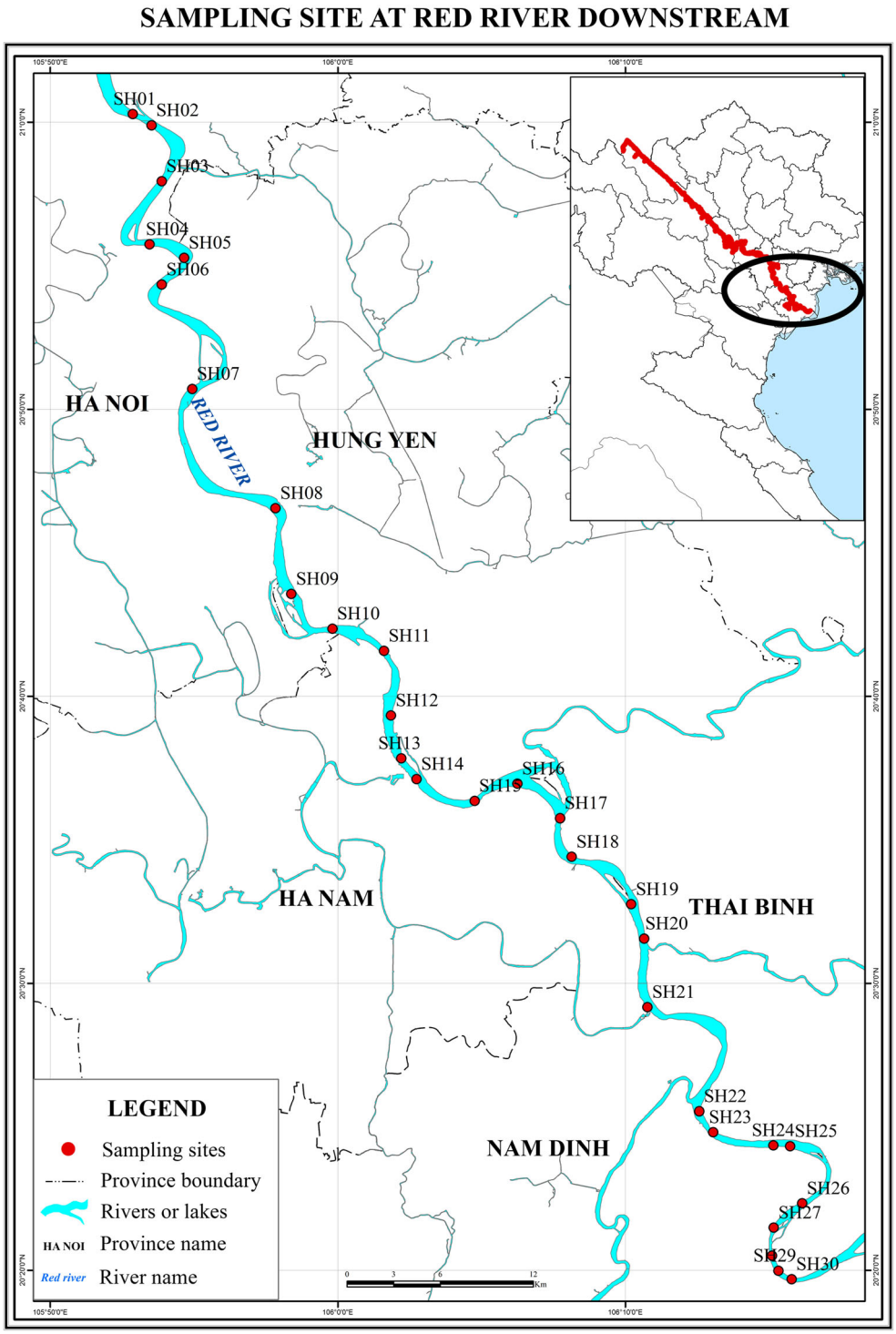


**Fig. 1** Map of sampling points in the Red River downstream area

5.5 to 6.0, respectively (see Supplement text for more detail). The overall water quality index was calculated by aggregating the individual WQI of each parameter selected.

$$WQI = \frac{WQI_I}{100} * \frac{\left(\prod_{i=1}^{m} WQI_m\right)^{\frac{1}{m}}}{100} * \left[\frac{1}{k}\sum_{i=1}^{k} WQI_{IV}\right] \quad (3)$$

where

$WQI_I$ the calculated WQI value for pH values (group 1);
$WQI_{III}$ the calculated WQI values for parameters in group 3;
$WQI_{IV}$ the calculated WQI values for parameters in group 4.

Based on the computed score of WQI, water quality is classified into six categories corresponding to the

**Table 1** Characteristics of pollution sources of the Red River downstream

| | Population | | Main waste sources | | |
|---|---|---|---|---|---|
| Province | Number (people) | Density (person/km$^2$) | Quantity (source) | Volume (m$^3$/day) | Waste sources |
| Ha Noi | 9,093,900 | 2410 | 60 | 456 | Hospitals, medical facilities |
| | | | 11 | 19,800 | Industrial zones, industrial clusters |
| | | | 95 | 1254 | Craft villages |
| | | | 130 | 520 | Livestock and agricultural production |
| Hung Yen | 1,269,090 | 1364 | 70 | 483 | Hospitals, medical facilities |
| | | | 5 | 21,000 | Industrial zones, industrial clusters |
| | | | 10 | 417 | Craft villages |
| | | | 81 | 405 | Livestock and agricultural production |
| Ha Nam | 854,469 | 991 | 138 | 800 | Hospitals, medical facilities |
| | | | 9 | 31,700 | Industrial zones, industrial clusters |
| | | | 60 | 2500 | Craft villages |
| | | | 50 | 298 | Livestock and agricultural production |
| Thai Binh | 1,942,000 | 1259 | 81 | 600 | Hospitals, medical facilities |
| | | | 4 | 4800 | Industrial zones, industrial clusters |
| | | | 62 | 2510 | Craft villages |
| | | | 48 | 345 | Livestock and agricultural production |
| Nam Dinh | 1,780,865 | 1076 | 124 | 970 | Hospitals, medical facilities |
| | | | 4 | 9896 | Industrial zones, industrial clusters |
| | | | 15 | 662 | Craft villages |
| | | | 89 | 352 | Livestock and agricultural production |

symbol and colors to assess the water quality to meet the needs of use (Table 2).

## Remote sensing data and processing methods

The Sentinel-2 mission consists of two satellites (Sentinel-2A, launched on June 23, 2015 and Sentinel-2B, launched March 7, 2017) developed to support natural resources and environmental monitoring. Together they cover all Earth's land surfaces, large islands, and inland and coastal waters every 5 days (https://sentinel.esa.int/). It acquires images in 13 spectral bands in visible, NIR, and SWIR wavelengths along a 290-km orbital swath. The European Space Agency's Copernicus Program (ESA) provides free images in the range of 0.443-2190 nm with the spatial resolution of 10 m (bands no. 2, 3, 4, 8), 20 m (bands no. 5, 6, 7, 8a, 11, 12), and 60 m (bands no. 1, 9, 10).

In this study, we downloaded the accessible Sentinel-2B data from the European Space Agency (ESA) on April 19, 2019 (https://earthexplorer.usgs.gov/). The collected Sentinel-2B multispectral images were used to estimate the total suspended sediment and turbidity concentration. After collecting images, the Sentinel-2B spectral bands were synchronized to the exact spatial resolution of 10 m using the SNAP software. Since the atmosphere affected the acquisition characteristics from satellite images, optical remote sensing images need to be corrected to apply for an assessment of environmental quality. The original images were transformed from digital numbers (DN) to reflection images at the top of the atmosphere R*(TOA). Then, these results were converted to surface reflections through an atmospheric correction (Mobley 1999). Sentinel-2B data was radiometric corrected at level-1C (L1C) by the supplier. In this study, the atmospheric correction was performed by dark object subtraction (DOS) method (Chavez 1996). This method estimates the atmospheric contributions to a surface spectrum by measuring 20 homogeneous surfaces over a range of illumination conditions. After atmospheric correction, the Sentinel-2B image is geometrically corrected to the local coordinate system VN-2000.

The water reflectance values ($\rho_w$) were extracted from visible bands (bands 2, 3, 4) and a near-infrared band (band 8) of Sentinel-2B image. A regression model was built to show the relationship between the $\rho_w$ and the turbidity and total suspended sediment (TSS) concentration measured in situ. The concentrations of TSS and turbidity in water samples are divided into two groups: Most of the measurement results were applied for building the regression model (SH08-SH30) and several for evaluating the regression model's accuracy (SH01-SH07). The regression model with the highest correlation coefficient ($R^2$) would be selected to estimate the turbidity and TSS concentration for the entire study area. Besides, the root mean square error (RMSE) and mean absolute percentage error (MAPE) were typically used to assess the performance in conjunction with the $R^2$.

**Table 2** The WQI and status of water quality

| | pH | DO (mg/L) | ORP (mV) | Turbidity (FTU) | TSS (mg/L) | $Cl^-$ (mg/L) | COD (mg/L) | $NH_4^+$ (mg/L) | $NO_3^-$ (mg/L) | $NO_2^-$ (mg/L) | $PO_4^{3-}$ (mg/L) | As (μg/L) |
|---|---|---|---|---|---|---|---|---|---|---|---|---|
| Average | 8.16 | 7.86 | 217 | 14.5 | 50.3 | 4.37 | 80.8 | 0.123 | 1.16 | 0.044 | 0.071 | 3.28 |
| Min | 7.76 | 7.04 | 51.4 | 9.88 | 31.0 | 2.84 | 24.0 | 0.023 | 0.622 | 0.004 | 0.002 | 1.24 |
| Max | 9.52 | 8.58 | 494 | 24.2 | 84.0 | 6.95 | 216 | 0.230 | 2.75 | 0.089 | 0.320 | 4.52 |
| SD | 0.431 | 0.435 | 128 | 3.43 | 11.5 | 1.15 | 40.1 | 0.054 | 0.378 | 0.024 | 0.083 | 0.821 |
| QCVN 08-MT:2015 | 5.5-9.0 | ≥ 4 | - | - | 50 | 350 | 30 | 0.9 | 10 | 0.05 | 0.3 | 50.0 |

## Results and discussion

### Water quality parameters in the Red River downstream area

The analytical results of various water quality parameters in surface water samples taken from the Red River downstream area are presented Table 3. Accordingly, most of the measured values were below the permissible limit for irrigation water specified by the National Technical Regulation on Surface Water Quality. However, the COD values ranged from 24.0 to 216 (average 80.0) mg/L, indicating that the Red River water may be polluted with organic matter. At almost all stations except at SH18, SH19, and SH22, the COD values were 1.6 to 7.2 times higher than the permitting limit values of QCVN 08-MT:2015/BTNMT (column B1). Domestic wastewater in the Red River Delta area accounts for 23% of the domestic wastewater whole country because of the high population density in the study area (MONRE 2018). In addition, according to the survey results from the Departments of Natural Resources and Environment of Ha Noi, Hung Yen, Ha Nam, Thai Binh, and Nam Dinh provinces, the daily wastewater flows derived from agricultural and cattle activities were approximately 1920 $m^3$ per day that corresponded to the COD pollution load of about 5414 kg per day to the Red River water source. The high values of TSS at most of the sampling sites could be explained by the naturally large amount of alluvium of the Red River (MONRE 2018). The nitrite contents in the water samples taken from Ha Nam Province and Nam Dinh Province (SH17 to SH30) were higher than those measured in the samples from Hanoi City. This observation can be explained by the influence of agricultural and industrial activities on the water environment. According to a report from the Department of Natural Resources and Environment in 2019, the total volume of wastewater discharged into river water from several main resources in Ha Nam Province, Thai Binh Province, and Nam Dinh Province were 35.298 $m^3$, 8255 $m^3$, and 9880 $m^3$ per day, respectively (Table 2). The high pollution load of N-$NO_2^-$ in wastewater has been affecting the content of nitrite in the Red River water.

The WQI values indicate that almost all water samples taken from our study area are in good and medium condition, except for a few samples in very bad quality (Fig. 2). At locations where the WQI values were high, the river water can be used for irrigation and domestic purposes. According to the national report on the current state of the environment in 2018, the surface water quality of the Red River basin significantly fluctuated during the period 2014–2018 (MONRE 2018). In recent years (2016–2018), water quality in some main rivers tended to decline. In fact, at some sampling sites such as SH5, SH19, and SH20, low WQI values indicate very bad water quality, mainly due to high pH, TSS, and COD

**Table 3** Water quality parameters of surface water samples collected from the Red River downstream

| The WQI score | Water quality status | Visible color | Action/purpose of use |
|---|---|---|---|
| 91-100 | Excellent water quality | Green | Domestic water supply |
| 76-90 | Good water quality | Blue | Domestic usage |
| 51-75 | Moderate water quality | Yellow | Irrigation and equivalent purposes |
| 26-50 | Poor water quality | Orange | Transportation and equivalent purposes |
| 10-25 | Very poor water quality | Red | Emergency treatment before use |
| <10 | Extreme polluted water | Brown | Emergency treatment before use |

values. The Red River receives wastewater from multiple sources from its catchments. Domestic wastewater usually contains high levels of nutrients, suspended solids, and organic compounds, which are responsible for the decrease of WQI values (Hoang et al. 2016; MONRE 2018).

The principal component analysis and cluster analysis were applied to field data to estimate the impact of each water quality parameter on water quality and potential relationships between the samples. The first five principal components (PC) of the parameters obtained from the results of principal component analysis explained 74.11% of the total variance of the hydration dataset (Table 4). The PC1, which contained positive loading on DO (0.228), turbidity (0.916), TSS (0.928), $Cl^-$ (0.666), and $PO_4^{3-}$ (0.228) (explaining 23.11% of the total variance), showed that the study area's water quality might be affected by rural domestic wastewater and agriculture non-point source. The $PO_4^{3-}$ in water mainly originated from crop plantations and livestock farms through surface runoff (MONRE 2018). The PC2, which explained 18.88% of the total variance, indicated the correlation the $BOD_5$ (0.807), $NH_4^+$ (0.718), and $NO_2^-$ (0.356). The oxygen-consuming pollutants in PC2 were mainly derived from human sewage and agricultural wastewater. The PC3 and PC5, explaining 12.69% and 8.80 % of the total variance, were correlated with As (0.629) and pH (0.873) in water. The factor loading of As indicated that some heavy metals may be related to influences from agricultural activities using pesticides and industrial point sources around the Red River (Yang et al. 2020).

Cluster analysis provides information about groups of samples that may have effects from similar waste sources (see Fig. S1). The cluster of samples SH05, SH19, and SH20 with heavily polluted water quality is a group of sampling points affected by wastewater discharged from health facilities and some industrial zones. The sampling site clusters of SH16-SH18 and SH08 with moderate and good water quality have a similar source of contamination from sand mining areas, craft villages of producing stone, and brick factories around the river. The clusters, including SH23-SH26 and SH28 and SH29 with moderate water quality, are corresponding to sites close to some large industrial zones and some hospitals such as Nam Dinh General Hospital and Nam Dinh Endocrine Hospital. The classification of sampling sites in the whole research area based on cluster analysis suggests a reduction in sampling sites in the monitoring network without affecting the reliability of the results (Dabgerwal and Tripathi 2016).

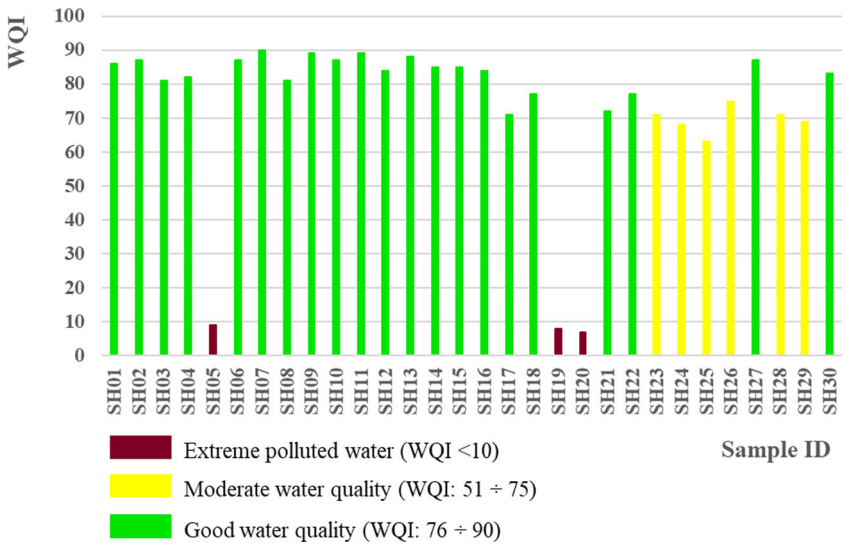


**Fig. 2** Water quality index (WQI) of surface water samples collected from the Red River downstream area

**Table 4** Factor loading in five principal components

| Variables | Principal component | | | | |
|---|---|---|---|---|---|
| | 1 | 2 | 3 | 4 | 5 |
| pH | 0.022 | −0.019 | −0.008 | 0.089 | **0.873** |
| Temperature | 0.366 | 0.053 | 0.181 | **0.841** | −0.118 |
| DO | 0.228 | −0.407 | 0.745 | 0.102 | 0.208 |
| Turbidity | **0.916** | 0.192 | 0.076 | 0.115 | 0.065 |
| TSS | **0.928** | 0.195 | 0.026 | 0.101 | 0.028 |
| COD | −0.249 | 0.093 | 0.755 | −0.423 | 0.031 |
| $BOD_5$ | 0.233 | **0.807** | −0.170 | −0.067 | 0.175 |
| $Cl^-$ | 0.666 | −0.242 | −0.224 | −0.207 | −0.175 |
| $NH_4^+$ | −0.066 | **0.718** | 0.009 | 0.168 | 0.008 |
| $NO_2^-$ | 0.299 | 0.356 | −0.498 | −0.159 | 0.190 |
| $NO_3^-$ | −0.116 | −0.651 | 0.180 | 0.222 | 0.289 |
| $PO_4^{3-}$ | 0.228 | 0.056 | 0.107 | −0.783 | −0.173 |
| As | 0.171 | −0.064 | 0.629 | 0.254 | −0.491 |
| Eigenvalues | 3.00 | 2.45 | 1.65 | 1.38 | 1.14 |
| % of variance | 23.11 | 18.88 | 12.69 | 10.62 | 8.80 |
| Cumulative | 23.11 | 41.99 | 54.68 | 65.30 | 74.10 |

Extraction method: principal component analysis

Rotation method: varimax with Kaiser normalization

Bold typeface: strong correlation coefficient

## Correlation between water quality parameters obtained by remote sensing and field monitoring

Figure 3 presents Sentinel-2B satellite image taken on April 19, 2019 with code number S2B_MSIL1C_20190419T032539_N0207_R018_T48QXH_20190419T080321. The water surface reflectance values ($\rho_w$) at visible bands (bands 2, 3, 4) and near-infrared band (band 8) of Sentinel-2B image of the study area are used to build regression model on the basis of total suspended sediment and turbidity concentration at 23 water sample points. In this study, we experiment with different regression models, including using only one band, using two bands, using 3 bands, and using all 4 visible and NIR bands of Sentinel-2B image. Next, the correlation coefficient ($R^2$) values in the regression models were compared to choose the optimal regression model for estimating the total suspended sediment and turbidity concentration (Espinoza Villar et al. 2013; Chelotti et al. 2019).

As a result, for both TSS and turbidity, the models with the best fit were using multiple bands ($R^2$ = 0,776 and 0.774; RMSE = 6.27 mg/L and 1.84 FTU; MAPE = 7.76% and 7.71% in respective). The slightly good results were also obtained with the band 2 that have $R^2$ = 0.721, RMSE = 0.004 mg/L, and MAPE = 8.74% for TSS, $R^2$ = 0.700, RMSE = 0.004 FTU, and MAPE = 8.65% for turbidity. The remaining models with a single band, two bands, and three bands were no good fit ($R^2 < 0.50$). Thus, three linear regression parameters ($R^2$, RMSE, and MAPE) indicated the good relationships for TSS, turbidity, and $\rho_w$ multiple linear regressions using four Sentinel-2B multispectral bands. Therefore, the multiple regression models that the dependent variable was TSS or turbidity and the independent variables were $\rho_w$ extracted from four Sentinel-2B multispectral bands (three visible bands and near-infrared band) were used to predict TSS and turbidity values at whole river region. The linear equation is shown below:

$$\text{TSS}\left(\frac{\text{mg}}{\text{L}}\right) = 1320,282B_2 - 336,432B_3 + 950,579B_4 - 30,350B_8 - 160,679 \quad (4)$$

$$\text{Turbidity (FTU)} = 384,681B_2 - 131,027B_3 + 330,741B_4 - 24,619B_8 - 46,770 \quad (5)$$

where $B_2$, $B_3$, $B_4$, and $B_8$ are the spectral reflectance values at blue (band 2), green (band 3), red (band 4), and near-infrared bands (band 8) of Sentinel-2B satellite images on April 19, 2019.

The TSS and turbidity datasets were predicted using the selected regression models for 30 sampling points (including seven samples for validation) with the mean and standard deviation of 50.0 mg/L and 10.9 mg/L (for TSS) and 14.7 and 3.11 FTU (for turbidity). The distribution of TSS and turbidity determined from the Sentinel-2B satellite image on April 19, 2019 in surface water in the Red River downstream is presented in Figs. 4 and 5, respectively. The satellite-derived TSS concentrations were from 33.7 to 78.0 mg/L, while turbidity content ranged from 8.95 to 22.8 FTU. Significantly, the values of TSS and turbidity were highest around SH18, with predicted values to be 78.0 mg/L and 22.8 (FTU), respectively. These results are similar to the distribution of TSS content and turbidity obtained from the analysis of real samples. Interestingly, the TSS content at most sampling sites determined from the Sentinel-2A satellite image is slightly smaller, while the turbidity values were gently higher than their values at the laboratory. The relative percent difference between both results ranged from 0.125 to 36.6% for TSS and 0.726 to 37.9% for turbidity. The results affirm that Sentinel-2B optical satellite images can be applied to calculate the concentration of TSS and turbidity with relatively high accuracy. In addition, when constructing a regression correlation between that value in the field and the predicted value, the values of RMSE and MAPE (Figure 6) for both TSS and turbidity were quite small, indicating good agreement between data obtained from two methods (Karaoui et al. 2019). The percentage error of 7.99 % and 14.3 % presented the acceptable average distance between the predicted and TSS measurement values and turbidity values. The small percentage error between predicted values and measurement values evidenced the effectiveness of the models.

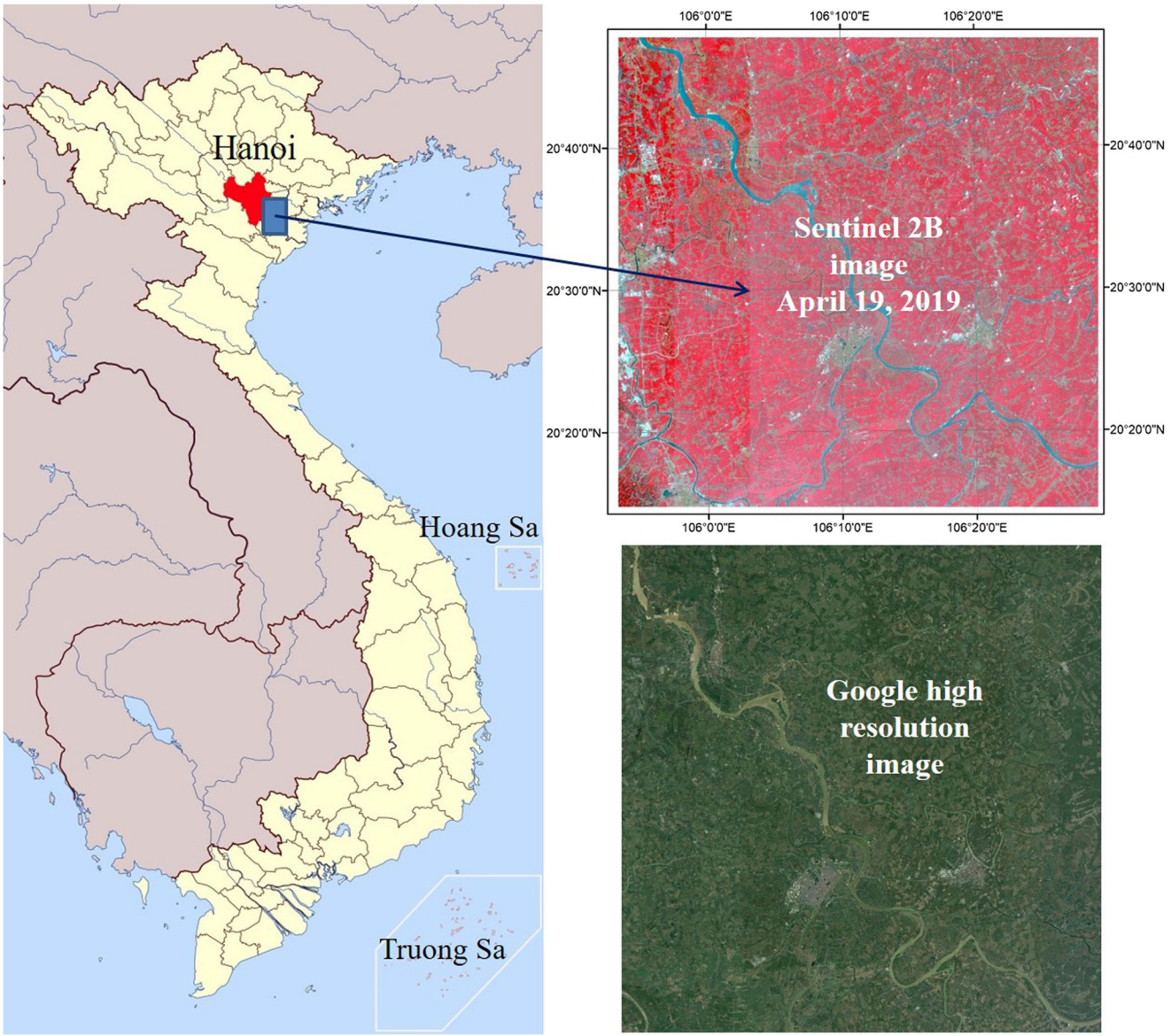


**Fig. 3** Sentinel-2B satellite image taken on April 19, 2019

In comparison, most previous studies built the linear regression models based on the spectral data and concentration of some quality parameters measured on-site. Then, $\rho_w$ or remote sensing reflectance ($R_{rs}$) from Sentinel-2 or Landsat imagery was used to retrieve water quality parameters (Potes et al. 2018; Karaoui et al. 2019; Yadav et al. 2019; Sent et al. 2021; Marinho et al. 2021). The researched results in the Negro River (Marinho et al. 2021) showed a good correlation between the $R_{rs}$ from in situ measurements and Sentinel-2 image ($R^2 > 0.80$, RMSE < 1.5 mg/L, and MAPE < 17%). The comparison between measurement water quality parameters and the reflectance in each sampling location at Marias Reservoir was used to investigate the relation between bands and laboratory analysis results at Bin EI Reservoir with $R^2$ greater than 0.52 and RMSE smaller than 1.024 mg/L (Karaoui et al. 2019). Besides, the measured values of field water quality parameters were both the input parameters for the regression models and the variance to test different algorithms for quality water parameters retrieval from Sentinel-2 data (Pizani et al. 2020). Pizani et al. (2020) produced multiple regression models that used the spectral reflectance bands from both Sentinel-2 sensor and Landsat-8 sensor at Três Marias Reservoir. Similar to this study, the values of R2, RMSE, and MAPE obtained from the regression model for Sentinel-2 images at Três Marias Reservoir were 0.78, 0.16, and 0.13, respectively. This evidence revealed that using a part of the

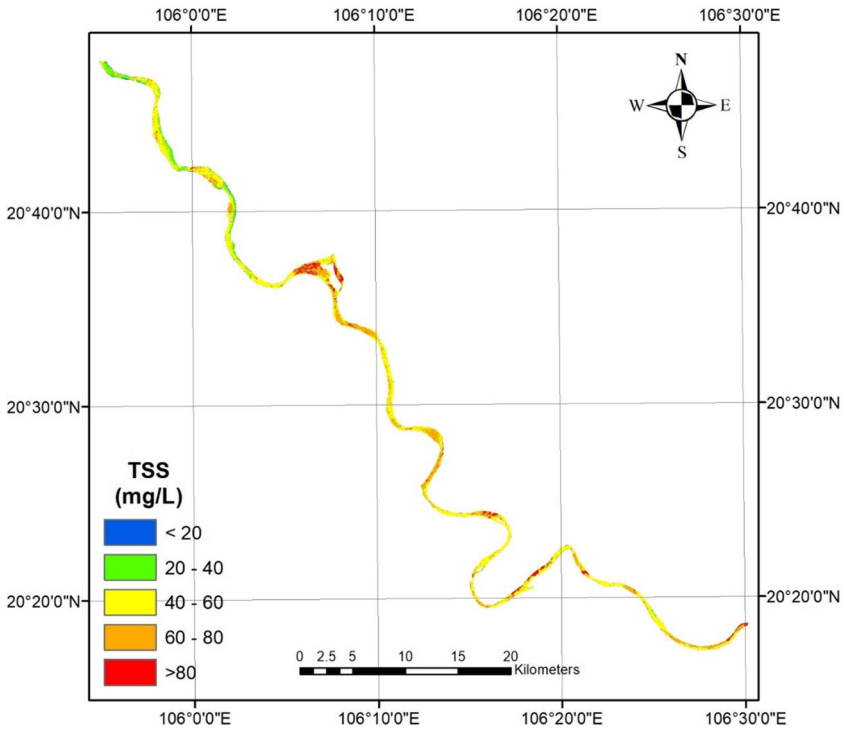


**Fig. 4** Spatial distribution of TSS concentrations in surface water of the Red River downstream area

experimental dataset of water quality parameters as the input data for the regression model in the remote sensing method will save the cost of measuring surface water reflectance in situ. Therefore, the field monitoring method and remote sensing method were combined to estimate the water quality parameters, which will save environmental monitoring costs and obtain the dataset with the high frequency of time and spatial.

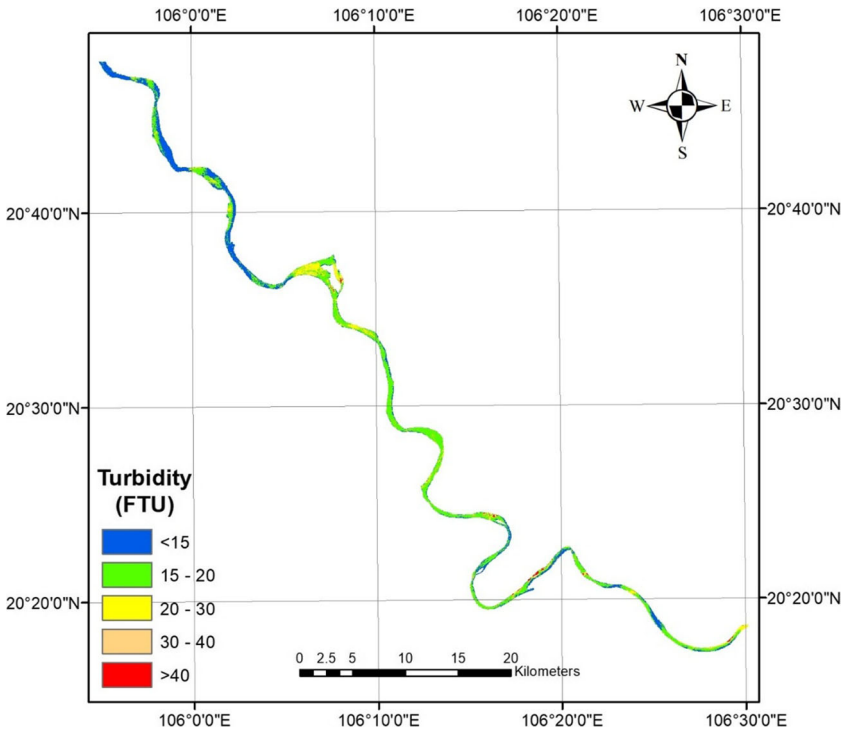


**Fig. 5** Spatial distribution of turbidity in surface water of the Red River downstream area

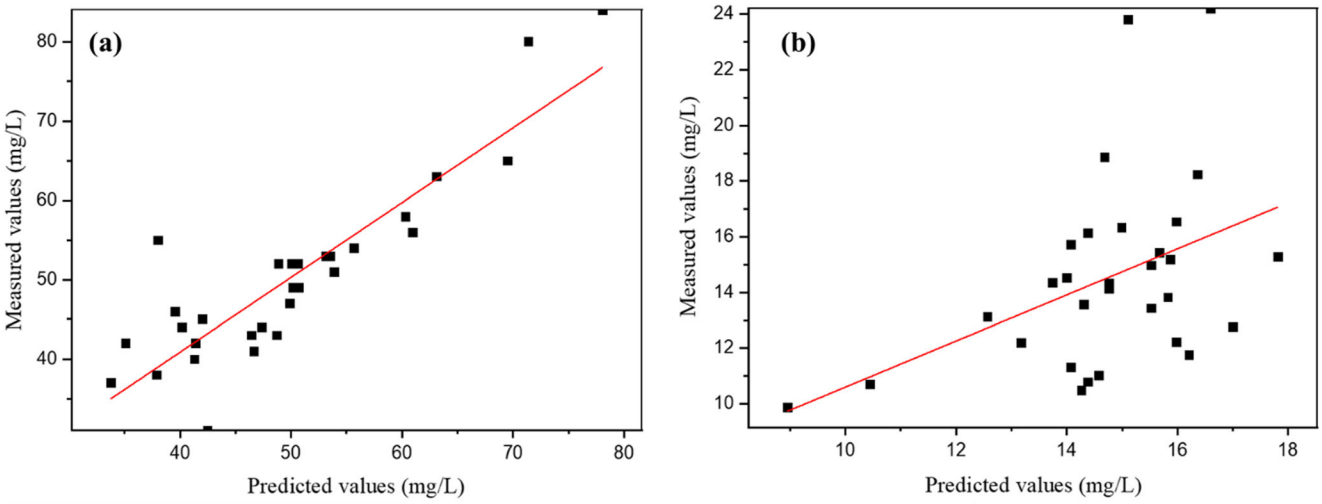


| | R-Square ($R^2$) | Root-MSE (RMSE) | MAPE (%) |
|---|---|---|---|
| TSS | 0.776 | 6.27 | 7.76 |
| Turbidity | 0.774 | 1.84 | 7.71 |

**Fig. 6** Correlation between predicted and measured values of **a** turbidity and **b** TSS concentrations in surface water of the Red River downstream area

## Conclusion

In the present study, we utilized field monitoring and remote sensing data to develop an effective method for the evaluation of turbidity and TSS concentrations in the surface water of river basins. Our method showed several advantages such as diverse spectra, good spatial resolution, short update time, and free support. The Sentinel-2 optical satellite images can be used to monitor certain parameters of water quality. Significant correlations between the predicted and measured values of TSS concentrations ($R^2$ = 0.776) and turbidity ($R^2$ = 0.774) were observed. Our analytical results show that TSS and turbidity values tend to increase toward the downstream, implying a decrease in water quality. However, the WQI values in almost all sampling stations indicate good water conditions. Besides, the accurate mapping of water quality parameters can be exploited to obtain the general idea of their concentration variation due to their high impacts on the water quality state. Furthermore, the results obtained in the study should be a useful information source, which could be used to monitor measurements and manage surface water in river basins.

**Supplementary Information** The online version contains supplementary material available at https://doi.org/10.1007/s11356-021-16730-0.

**Author contribution** All authors contributed to the study conception and design. Material preparation, data collection, and analysis were performed by Trinh Thi Tham, Trinh Le Hung, Trinh Thi Thuy, Vu Thi Mai, Le Thi Trinh, and Chu Vu Hai. The first draft of the manuscript was written by Trinh Thi Tham and Trinh Le Hung, and all authors commented on previous versions of the manuscript. Supervision, conceptualization, and writing—review and editing were performed by Tu Binh Minh. All authors read and approved the final manuscript.

**Funding** This research was funded by the Vietnam Ministry of Natural Resource and Environment (MONRE) (grant number TNMT 2018.02.15).

**Data availability** All data generated or analyzed during this study are included in this published article and its supplementary information files.

## Declarations

**Ethics approval and consent to participate** Not applicable.

**Consent for publication** Not applicable.

**Competing interests** The authors declare no competing interests.

## References

Alastal KM, Alagha JS, Abuhabis AA, Ababou R (2015) Groundwater quality assessment using water quality index (WQI) approach: Gâz Coastal aquifer case study. Journal of Engineering Research and Technology 2(1):80–86

Baird RB, Eaton AD, Rice EW (2017) Standard methods for the examination of water and wastewater. American Public Health Association, American Water Works Association, Water Environment Federation

Bresciani M, Giardino C, Stroppiana D, Dessena MA, Buscarinu P, Cabras L, Schenk K, Heege T, Bemet H, Bazdanis G, Tzimas A (2019) Monitoring water quality in two damment reservoirs from multispectral satellite data. European Journal of Remote Sensing 52(54):113–122

Brown R.M., McClelland N.I., Deininger R.R., O'Connor M.F. (1971) A water quality index - crashing the psychological barrier. Indicators of Environmental Quality, pp.173-182.

Cao TS, Nguyen THG, Trieu PT, Nguyen HN, Nguyen TL, Vo HC (2020) Assessment of Cau river water quality assessment using a

combination of water quality and pollution indices. Journal of Water Sullly: Research and Technology-Aqua 69(2):160–172
CCME (2001) Canadian environmental quality guidelines for the protection of aquatic life. CCME water quality index: technical report, 1.0.
Chavez PS (1996) Image-based atmospheric corrections – revisited and improved. Photogrammetric Engineering and Remote Sensing 62(9):1025–1036
Chelotti GB, Martinez JM, Roig HL, Olivietti D (2019) Space-temporal analysis of suspended sediment in low concentration reservoir by remote sensing. Brazil Journal of Water Resources 24:1–15
Chen Z, Hanson JD, Curran PJ (1991) The form of the relationship between suspended sediment concentration and spectral reflectance: its implications for the use of Daedalus 1268 data. International Journal of Remote Sensing 12(1):215–222
Chen Z, Curran PJ, Hanson JD (1992) Derivative reflectance spectroscopy to estimate suspended sediment concentration. Remote Sensing of Environment 40(1):67–77
Dabgerwal DK, Tripathi SK (2016) Assessment of surface water quality using hierarchical cluster analysis. International Journal of Environment 5(1):31–43
Dekker A, Zamurovic-Nenad Z, Hoogenboom H, Peters S (1996) Remote sensing, ecological water quality modelling and in situ measurements: a case study in shallow lakes. Hydrologycal Science Journal 41:531–547
Doxaran D, Froidefond JM, Lavender S, Castaing P (2007) Spectral signature of highly turbid waters application with SPOT data to quantify suspended particulate matter concentrations. Remote Sensing of Environment 81:149–161
Ennaji W, Barakat A, Karaoui I, El Baghdadi M, Arioua A (2018) Remote sensing approach to assess salt-affected soils in the northeast part of Tadla plain, Morocco. Geology, Ecology and Landscapes 2(1):22–28
Espinoza Villar R, Martinez J-M, Le Texier M, Guyot J-L, Fraizy P, Meneses PR, de Oliveira E (2013) A study of sediment transport in the Madeira River, Brazil, using MODIS remote-sensing images. Journal of South American Earth Sciences 44:45–54
Gholizadeh MH, Melesse AM, Reddi L (2016) A comprehensive review on water quality parameters estimation using remote sensing techniques. Sensors 16(8):2–43
Giardino C, Bresciani M, Villa P, Martinelli A (2010) Application of remote sensing in water resource management: the case study of Lake Trasimeno, Italy. Water resources management 24(14):3885–3899
Guzman VR, Santaella FG (2009) Using MODIS 250m imagery to estimate total suspended sediment in a tropical open bay. International Journal of Systems Applications, Engineering & Development 3(1):36–44
He W (2008) Water quality monitoring in slightly – polluted body through remote sensing – a case study in Guanting Reservoir Beijing, China. Frontiers of Environmental Science & Engineering in China 2(2):163–171
Hoang TTH, Nguyen TK, Le TPQ, Dang DK, Duong TT (2016) Assessment of the water quality downstream of Red River in 2015 (Vietnam). Journal of Vietnamese Environment 8(3):167–172
Horton RK (1965) An index number system for rating water quality. Journal of Water Pollution Control Federation 37(3):300–306
Hung TL, Tarasov MK (2016) Evaluation of suspended matter concentrations in surface water of the Tri An water reservoir (Vietnam) using the remote sensing data. Moscow State University Bulletin Serial 5 – Geography(2):38–43
Karaoui I, Arioua A, Boudhar A, Hssaisoune M, Mouatassime SE, Ouhamchich KA, Elhamdouni D, Idrissi AEA, Nouaim W (2019) Evaluating the potential of Sentinel-2 satellite images for water quality characterization of artificial reservoirs: the Bin El Ouidane Reservoir case study (Morocco). Meteorology Hydrology and Water Management 7(1):31–39
Ke LC, Tran HTV, Liem VH, Tuong TN, Duyen PT (2015) Assessment of surface water pollutant models of estuaries and coastal zone of Quang Ninh – Hai Phong using Spot-5 images. Geodesy and Cartography 64(1):29-42
Kiselev V, Bulgarelli B, Heege T (2015) Sensor independent adjacency correction algorithm for coastal and inland water systems. Remote Sensing of Environment 157:85–95
Knaeps E, Dogliotti A, Raymaekers D, Ruddick K, Sterchx S (2012) In situ evidence of non-zero reflectance in the OLCI 1020 nm band for a turbid estuary. Remote Sensing of Environmen 120:133–144
Liou SM, Lo SL, Wang SH (2004) A generalized water quality index for Taiwan. Environmental Monitoring and Assessment 96:35–32
Luu TNM, Garnier J, Billen G, Orange D, Nemery J, Le TPQ, Tran HT, Le LA (2010) Hydrological regime and water budget of the Red River Delta (Northern Vietnam). Journal of Asian Earth Sciences 37:219–228
Marinho RR, Harmel T, Martinez JM, Filizola Junior NP (2021) Spatiatemporal dynamics of suspended sediments in the Negro River, Amazon Basin, from in situ and Sentinel-2 remote sensing data. International Journal of Geo-Information 10(2):86
Ministry of Natural Resources and Environment (2018) Vietnam: National State of Environment Report 2018 on water resources.
Mobley C (1999) Estimation of the remote-sensing reflectance from above-surface measurements. Applied Optics 38:7442–7455
Moran MS (1992) Evaluation of simplified procedures for retrieval of land surface reflectance factors from satellite sensor output. Remote Sensing of Environment 41:169–184
National Centre for Water Resources Planning and Investigation (NAWAPI), Ministry of Natural Resources and Environment (MONRE) (2016) The water resources planning in Hong-Thai Binh River basin.
Nguyen TTH, Zhang W, Li Z, Li J, Ge C, Liu J, Bai X, Feng H, Yu L (2016) Assessment of heavy metal pollution in Red River surface sediments, Viet Nam. Marine Pollution Bulletin 113(1-2):513–519
Nguyen TTH, Koike K, Mai TN, Canh BD, Thao NTP, Parsons M (2017a) Landsat 8/OLI two bands ratio algorithm for chlorophyll-a concentration mapping in hypertrophic waters: an application to West Lake in Hanoi (Vietnam). IEEE Journal of Selected Topics in Applied Earth Observations and Remote Sensing 10(11):4919–4929
Nguyen TTH, Nguyen TPT, Koike K, Mai TN (2017b) Selecting the best band ratio to estimate chlorophyll-a concentration in a tropical freshwater lake using sentinel 2A images from a case study of Lake Ba Be (Northern Vietnam). ISPRS International Journal of Geo-Information 6(9):290
Pham QV, Nguyen TTH, Pahlevan N, Oanh LT, Nguyen TB, Nguyen NT (2018) Using Landsat-8 images for quantifying suspended sediment concentration in Red River (Northern Vietnam). Remote Sensing 10(11):1841
Pizani FMC, Maillard P, Ferreira AFF, de Amorim CC (2020) Estimation of water quality in a reservoir from Sentinel-2 MSI and Landsat-8 OLI sensors. ISPRS Annals of Photogrammetry, Remote Sensing and Spatial Information Sciences 3:401–408
Potes M, Rodrigues G, Penha AM, Novais MH, Costa MJ, Salgado R, Morais MM (2018) Use of Sentinel 2-MSI for water quality monitoring at Alqueva reservoir, Portugal. Earth Observation for Integrated Water and Basin Management, IAHS 380:73–79
Richter, R. (2009) Atmospheric/topographic correction for satellite imagery. DLR report DLR-IB 565-01/09, Wessling, Germany.
Ritchie JC, Schiebe FR, McHenry JR (1976) Remote sensing of suspended sediments in surface waters. Journal of American Society of Photogrammetry 42(12):1539–1545
Ritchie JC, Cooper CM, Yongqing J (1987) Using Landsat multispectral scanner data to estimate suspended sediments in Moon Lake, Mississippi. Remote Sensing of Environment 23:65–81

Ritchie JC, Cooper CM, Schiebe FR (1990) The relationship of MSS and TM digital data with suspended sediments, chlorophyll, and temperature in Moon Lake, Mississippi. Remote Sensing of Environment 33:137–148

Sargaonkar A, Deshpande V (2003) Development of an overall index of pollution for surface water based on a general classification scheme in Indian context. Environmental Monitoring and Assessment 89: 43–67

Sent G, Biguino B, Favareto L, Cruz J, Sá C, Dogliotti AI, Palma C, Brotas V, Brito AC (2021) Deriving water quality parameters using Sentinel-2 imagery: a case study in the Sado Estuary, Portugal. Remote Sensing 13:1043

Shweta T, Bhavtosh S, Prashant S, Rajendra D (2013) Water quality assessment in terms of water quality index. American Journal of Water Resources 1(3):34–38

Sliwka-Kaszyńska M, Kot-Wasik A, Namieśnik J (2003) Preservation and storage of water samples. Critical Reviews in Environmental Science and Technology 33(1):31–44

Tran QB, Pham AD (2020) Developing a water quality index (WQI) for river resources management in Kien Giang province, Vietnam. IOP Conference Series: Earth and Environmental Science 444(012054)

Tsegaye T, Sheppard D, Islam KR, Johnson A, Tadesse W, Atalay A, Marzen L (2006) Development of chemical index as a measure of in-stream water quality in response to land-use and land cover changes. Water, Air, and Soil Pollution 174:161–179

Yadav S, Yamashiki Y, Susaki J, Yamashita Y, Ishikawa K (2019) Chlorophyll estimation of lake water and coastal water using Landsat-8 and Sentinel-2A satellite. The International Archives of the Photogrammetry, Remote Sensing and Spatial Information Sciences 42(3/W7):77–82

Yang W, Zhao Y, Wang D, Wu H, Lin A, He L (2020) Using principal components analysis and IDW interpolation to determine spatial and temporal changes of surface water quality of Xin'anjiang River in Huangshan, China. International Journal of Environmental Research and Public Health 17:2942

Yepez S, Laraque A, Martinez J, De Sa J, Carrera J, Castellanos B, Gallay M, Lopez J (2018) Retrieval of suspended sediment concentrations using Landsat-8 OLI satellite images in the Orinoco River (Venezuela). Comptes Rendus Geoscience 350(1-2):20–30